High Efficiency Desulfurization of Synthesis Gas

Annual Report

September 2001 – August 2002

Kwang-Bok Yi
Elizabeth J. Podlaha
Douglas P. Harrison

November 2002

DE-PS26-00FT40813

Gordon A. and Mary Cain Department of Chemical Engineering
Louisiana State University
Baton Rouge, LA 70803

DISCLAIMER

ABSTRACT

Mixed metal oxides containing CeO_2 and ZrO_2 are being studied as high temperature desulfurization sorbents capable of achieving the DOE Vision 21 target of 1 ppmv or less H_2S. The research is justified by recent results in this laboratory that showed that reduced CeO_2, designated CeO_n ($1.5 < n < 2.0$), is capable of achieving the 1 ppmv target in highly reducing gas atmospheres. The addition of ZrO_2 has improved the performance of oxidation catalysts and three-way automotive catalysts containing CeO_2, and should have similar beneficial effects on CeO_2 desulfurization sorbents.

An electrochemical method for synthesizing CeO_2-ZrO_2 was developed and the products were characterized by XRD and TEM during year 01. Nanocrystalline particles having a diameter of about 5 nm and containing from approximately 10 mol% to 80 mol% ZrO_2 were prepared. XRD showed the product to be a solid solution at low ZrO_2 contents with a separate ZrO_2 phase emerging at higher ZrO_2 levels. Unfortunately, the quantity of CeO_2-ZrO_2 that could be prepared electrochemically was too small to permit full testing in our desulfurization reactor.

Also during year 01 a laboratory-scale fixed-bed reactor was constructed for desulfurization testing. All components of the reactor and analytical systems that may be exposed to low concentrations of H_2S are constructed of quartz, Teflon, or silcosteel. Reactor product gas composition as a function of time is determined using a Varian 3800 gas chromatograph equipped with a pulsed flame photometric detector (PFPD) for measuring low H_2S concentrations (<~10 ppmv) and a thermal conductivity detector (TCD) for higher concentrations of H_2S.

Larger quantities of CeO_2-ZrO_2 mixtures from other sources, including mixtures prepared in this laboratory using a coprecipitation procedure, have been obtained. Characterization and desulfurization testing of these sorbents began in year 02 and is continuing. To properly evaluate the effect of ZrO_2 addition on desulfurization capability, the physical properties of the sorbent mixtures must be similar. That is, a CeO_2-ZrO_2 mixture from source A would not necessarily be superior to pure CeO_2 from source B if the properties were dissimilar. Therefore, current research is concentrating on CeO_2 and CeO_2-ZrO_2 mixtures prepared in this laboratory using the coprecipitation procedure. The structure of these sorbents is similar and the effect of ZrO_2 addition can be separated from other effects.

X-ray diffraction tests of the sorbents prepared in house have confirmed the existence of a solid solution of ZrO_2 in CeO_2. Reduction tests using an electrobalance reactor have confirmed that CeO_2-ZrO_2 mixtures are more easily reduced than pure CeO_2. Reduction of CeO_2-ZrO_2 begins at a lower temperature and the final value of n in CeO_n ($1.5 < n < 2.0$) is smaller in CeO_2-ZrO_2 than in pure CeO_2. 700°C desulfurization tests have shown that both CeO_2 and CeO_2-ZrO_2 sorbents are capable of reaching the target sub-ppmv H_2S level in highly reducing gases. Some CeO_2-ZrO_2 sorbents have successfully removed H_2S to the minimum detectable limit of the PFPD detector, approximately 100 ppbv.

TABLE OF CONTENTS

LIST OF FIGURES

LIST OF TABLES

EXECUTIVE SUMMARY

The DOE Vision 21 program requires more stringent control of H_2S concentration in coal-derived synthesis gas to be used for certain applications. Previous target levels of about 20 ppmv H_2S suitable for electric power generation using an integrated gasification combined cycle process (IGCC) have been replaced by H_2S targets of 1 ppmv or less required for fuel cell and other catalytic processes.

Zinc-based sorbents developed for IGCC applications are not capable of achieving the Vision 21 target at high temperatures. Reduced cerium oxide, CeO_n ($1.5 < n < 2.0$), has recently been shown to be capable of reducing H_2S to less than 1 ppmv at temperatures near 700°C in gas atmospheres having considerably greater reducing power than typical coal-derived gases. Related research in oxidation catalysis and three-way automotive catalysis has shown that catalyst performance is improved by the addition of ZrO_2 to the CeO_2. The reasons given for the improved performance, including increased oxygen exchange capacity, should also result in improved desulfurization performance.

This research project consists of two major activities – the electrochemical synthesis and characterization of CeO_2-ZrO_2 materials, and high temperature desulfurization tests using CeO_2-ZrO_2 sorbents. The electrochemical synthesis was the primary focus during year 01 and results were presented in the previous annual report (Mukherjee et al. 2001). Nanocrystalline powders of approximately 5 nm grain diameter and containing from 10 mol% to 80 mol% ZrO_2 were deposited at an electrode surface using the cathodic generation of base method. Conditions required for the production of desired solid solutions of CeO_2-ZrO_2 having a fluorite-type structure were identified. A separate ZrO_2 phase was formed at high ZrO_2 concentration. Heat treatment at 700°C for as long as 106 hrs at 700°C produced no phase separation, but the crystallite size increased from 5 nm to 14.5 nm. Unfortunately, the quantities of CeO_2-ZrO_2 that could be produced using this method were too small to permit realistic desulfurization testing, and other sources of CeO_2-ZrO_2 sorbents have been pursued.

A laboratory-scale fixed-bed reactor having a capacity of about 15 g of solid was constructed during year 01 for desulfurization testing. In order to avoid interaction between low concentrations of H_2S and stainless steel, all components of the reactor and analytical systems that may be exposed to low H_2S concentrations are constructed of quartz, Teflon, or silcosteel. Reactor product gas composition as a function time is determined using a Varian 3800 gas chromatograph purchased for this project with LSU matching funds. The chromatograph is equipped with a pulsed flame photometric detector (PFPD) for measuring low H_2S concentrations ($< \approx 10$ ppmv) and a thermal conductivity detector (TCD) for higher concentrations of H_2S.

Larger quantities of CeO_2 and CeO_2-ZrO_2 suitable for desulfurization testing have been obtained from a number of sources, including materials prepared in this laboratory using a coprecipitation procedure. Characterization and desulfurization testing of these sorbents is currently being carried out. X-ray diffraction tests have confirmed the existence of a solid solution of ZrO_2 in CeO_2. Reduction tests using an electrobalance

reactor have confirmed that CeO_2-ZrO_2 mixtures are more easily reduced than pure CeO_2. Reduction begins at a lower temperature and the final value of n in CeO_n ($1.5 < n < 2.0$) is smaller in CeO_2-ZrO_2 than in pure CeO_2.

Early desulfurization tests proved that to properly evaluate the effect of ZrO_2 additions, the sorbents must have similar physical properties. That is, a CeO_2-ZrO_2 mixture from one source would not necessarily have superior desulfurization capability than pure CeO_2 from another source unless the two sorbents had similar physical properties. Therefore, current desulfurization research is concentrating on CeO_2 and CeO_2-ZrO_2 prepared in this laboratory using a coprecipitation procedure. The structure of these sorbents is similar and the effect of ZrO_2 addition can be separated from other effects.

Desulfurization tests completed to date have been restricted to 700°C using a highly reducing gas. Both pure CeO_2 and CeO_2-ZrO_2 mixtures are capable of achieving the Vision 21 target at these conditions. However, prebreakthrough H_2S concentrations using CeO_2-ZrO_2 mixtures are consistently lower, and concentrations below the PFPD detection limit of about 10 ppbv have been found using certain CeO_2-ZrO_2 mixtures.

I. INTRODUCTION

Research relating to the high temperature desulfurization of coal-derived gas has been a major component of the DOE fossil energy program for a number of years. In the past, the primary objective was to reduce H_2S concentration to levels required for electric power generation using integrated gasification combined cycles (IGCC), approximately 20 ppmv. Desulfurization processes for this application using zinc-based sorbents have progressed to the demonstration stage. The new DOE Vision 21 program, however, requires much more stringent sulfur control measures. Sulfur levels equal to or less than 1 ppmv are required for fuel cells and certain synthesis gas catalytic processes. New sorbents are needed to meet these more stringent sulfur limits.

Recent research in this laboratory (Zeng et al. 1999, Zeng et al. 2000) showed that reduced cerium oxide, designated CeO_n ($1.5 < n < 2.0$), is capable of reducing H_2S from 1 mol% to less than 1 ppmv at temperatures near 700°C in highly reducing gas compositions. However, the product compositions from gasifiers currently available in the United States (Texaco, KRW, etc.) do not have the reducing power required to achieve significant CeO_2 reduction. The equilibrium H_2S content in contact with unreduced CeO_2 is well above the more stringent Vision 21 target levels.

The current research is investigating the desulfurization performance of mixed oxide sorbents of CeO_2-ZrO_2 with the objective of meeting Vision 21 target levels in less reducing gas compositions. The addition of ZrO_2 to CeO_2 has improved the performance of oxidation catalysts and three-way automotive catalysts. The improvement is attributed to increased reducibility and improved oxygen mobility resulting from the addition of ZrO_2, factors that should also improve desulfurization performance.

1.1. High Temperature Gas Desulfurization

High temperature desulfurization of coal-derived gas is based on the noncatalytic gas-solid reaction between H_2S and an appropriate metal oxide. The reaction may be written generically as follows

$$H_2S(g) + MeO(s) \leftrightarrow H_2O(g) + MeS(s) \quad (1)$$

The generic reaction for the regeneration of the metal sulfide is

$$MeS(s) + 1.5O_2(g) \leftrightarrow MeO(s) + SO_2(g) \quad (2)$$

For economic reasons, the sorbent must maintain activity through many sulfidation-regeneration cycles. A number of metals including Zn, Fe, Mn, Cu, and Ca have been studied but most of the recent research has focused on Zn-based materials, including ZnO (e.g., Gibson and Harrison 1980), $ZnFe_2O_4$ (e.g., Focht et al. 1988), and $ZnO{\bullet}xTiO_2$ (e.g., Woods et al. 1990).

Harrison (1998) has discussed the advantages and disadvantages of zinc-based sorbents. Advantages include favorable desulfurization thermodynamics, rapid kinetics, large stoichiometric sulfur capacity (39 g S/100 g ZnO), and relatively low cost. Disadvantages include the tendency for ZnO to be reduced to volatile metallic Zn at high temperature, the highly exothermic nature of the regeneration reaction, and the possible formation of $ZnSO_4$ during regeneration. The tendency for ZnO reduction followed by Zn vaporization can be moderated, but not eliminated, by the addition of TiO_2 to form the mixed metal oxide $ZnO{\bullet}xTiO_2$. However, TiO_2 addition increases the sorbent processing cost and reduces the sulfur capacity. Dilute O_2 is used to control temperature during regeneration, but this causes dilute SO_2 to be produced and complicates the ultimate sulfur control problem. $ZnSO_4$, because of its large molar volume, has been identified as a cause of rapid sorbent deterioration in multicycle tests, and careful control of temperature and the partial pressures of O_2 and SO_2 are required to prevent its formation.

The performance of CeO_2 as a high temperature desulfurization sorbent was recently studied in this laboratory (Zeng et al. 1999, Zeng et al. 2000). H_2S concentrations were reduced from 1 mol% (10,000 ppmv) to 1 ppmv or less at temperatures in the range of 650°C to 800°C in highly reducing atmospheres. Reduction of CeO_2 to oxygen-deficient CeO_n ($n < 2$) was the key in achieving low H_2S concentrations. The sulfided product, Ce_2O_2S, was easily regenerated using SO_2 with sulfur liberated in elemental form. Preliminary multicycle tests (25 complete cycles) showed no evidence of significant sorbent deterioration.

The complete cycle using cerium sorbent consists of three steps – reduction, sulfidation, and regeneration – as shown by the following reactions.

Reduction: $$CeO_2(s) + (2\text{-}n)H_2(g) \leftrightarrow CeO_n(s) + (2\text{-}n)H_2O(g) \quad (3)$$

Sulfidation: $$2CeO_n(s) + H_2S(g) + (2\text{-}3n)H_2(g) \leftrightarrow Ce_2O_2S(s) + 2(n\text{-}1)H_2O(g) \quad (4)$$

Regeneration: $$Ce_2O_2S(s) + SO_2(g) \leftrightarrow 2CeO_2(s) + S_2(g) \quad (5)$$

The ultimate degree of reduction, i.e., the equilibrium value of n, depends on temperature and the oxygen partial pressure of the reducing gas, as described by Bevan and Kordis (1964) and Sorensen (1976). Reduction experiments in this laboratory using an electrobalance reactor have shown that the level of reduction, i.e., the experimental value of n, is in close agreement with the results of Bevan and Kordis. Unfortunately the oxygen partial pressure in the product gas from typical U.S coal gasifiers (Texaco and KRW) is too large to achieve significant CeO_2 reduction.

The current research is examining the addition of ZrO_2 to CeO_2 in the hope that reduction to CeO_n can be more easily accomplished. The expected benefits are based on results from recent research in the areas of oxidation and automotive catalysis summarized in the following section.

1.2. Ceria-Zirconia Catalyst Research

CeO_2 serves an important role in three-way automotive catalysts (TWC) by regulating the gas phase oxygen pressure. During fuel rich operation, CeO_2 is reduced to CeO_n and the oxygen released assists in the oxidation of CO and hydrocarbons to CO_2. Under fuel lean conditions CeO_n is re-oxidized to CeO_2 and removal of oxygen from the gas phase assists in the reduction of NO_x to N_2. In oxidation catalysis, the CeO_2 is reduced to CeO_n by surface adsorbed species as they are oxidized to CO_2, and the CeO_n is then re-oxidized to CeO_2 by oxygen from the gas phase.

Recent research has shown that the addition of ZrO_2 to CeO_2 enhances the redox reactions. Colon et al. (1998) state that the addition of ZrO_2 enhances the oxygen mobility within the crystal and improves the catalyst thermal stability at 1000^{o}C. Zamar et al. (1995) discuss the enhanced oxygen storage and release capacity of CeO_2-ZrO_2 mixtures used for CH_4 combustion. ZrO_2 was said to promote the formation of oxygen vacancies and increase the mobility of bulk oxygen. The 50% CH_4 conversion level was reached at a temperature 130^{o}C lower using $Ce_{0.8}Zr_{0.2}O_2$ compared to CeO_2 alone.

Hori et al. (1998) report an increase in reversibly stored oxygen by a factor of 1.7-2.5 for phase separated CeO_2-ZrO_2 compared to CeO_2 alone, and by a factor 0f 3-5 for solid solutions of CeO_2-ZrO_2. The optimum Zr concentration was 25 mol%, but performance was relatively insensitive to Zr loading between 15 mol% and 50 mol%. Bunluesin et al. (1997) found that addition of ZrO_2 slowed the catalyst deactivation rate for CO oxidation over a Ce-Pd catalyst. Deactivation without ZrO_2 was attributed to a large increase in crystallite size, and ZrO_2 was said to slow crystallite growth.

Trovarelli et al. (1997) and Cuif et al. (1996) discuss the improved performance of three-way automotive catalysts due to the addition of ZrO_2 to CeO_2. Trovarelli et al. state that the addition of ZrO_2 enhances the catalytic, textural, redox, and oxygen storage properties of ceria. Trovarelli (1996) and Ozawa (1997) have published recent reviews describing the beneficial effects of ZrO_2 addition.

These positive effects on the performance of CeO_2 catalysts associated with ZrO_2 addition – improved redox potential, increased oxygen mobility, higher oxygen exchange capacity, improved activity at lower temperature, and increased thermal stability – are the same factors needed to improve the performance of ceria-based desulfurization sorbents. Therefore, the objective of the current research is to demonstrate that ceria-zirconia sorbents are capable of achieving Vision 21 desulfurization goals in typical coal gas compositions.

The project is divided into two major activities – the electrochemical synthesis and characterization of CeO_2-ZrO_2 mixtures and high temperature desulfurization using CeO_2-ZrO_2 sorbents. Electrochemical synthesis and characterization and construction of a laboratory-scale fixed-bed reactor suitable for determining sub-ppmv H_2S concentrations were emphasized during year 01. These topics were described in detail in the previous annual report (Mukherjee et al. 2001) and only brief summaries are repeated

in this report. While the electrochemical synthesis work was successful, it proved to be impossible to produce sufficient quantities of material to properly evaluate the desulfurization potential. Therefore, CeO_2 and CeO_2-ZrO_2 materials from other sources, including materials synthesized at LSU using a coprecipitation process are being used for desulfurization studies.

2. ELECTROCHEMICAL SYNTHESIS AND CHARACTERIZATION OF CeO_2-ZrO_2

Switzer (1987) and Yanchun et al. (1995) have recently demonstrated the electrochemical synthesis of CeO_2 and ZrO_2, respectively, but there has been no previous work on the electrochemical preparation of CeO_2-ZrO_2 mixtures. In this study, the powders were co-deposited and the chemical composition, phase structure, and crystallite size of the mixture was studied as a function of the processing parameters. Conditions have been identified for producing ceria-zirconia mixtures that exhibit solid solutions of the fluorite-type structure, are nanocrystalline, and have about 25mol % zirconia.

2.1. Electrochemical Experimental

Figure 1 shows the two-compartment electrochemical cell employed in the powder synthesis. The anolyte and catholyte were separated by a glass frit A platinum mesh was used as the anode. The reference electrode was a saturated calomel electrode (SCE). An inverted, stationary, stainless steel shaft-disk electrode was used as described by Podlaha et al. (1997) with the electrode surface facing upwards in the electrolyte to avoid blockage of the electrode surface by trapped H_2 gas bubbles, produced from water and proton reduction. The stainless steel disc electrodes (AISI 304L) were embedded inside an epoxy resin such that only one side was exposed to the electrolyte. A thin, stainless steel shaft, encased in Teflon, was screwed into the disc-epoxy assembly. The shaft was threaded allowing electrical contact to the disc.

The electrolyte consisted of 0.5 M ammonium nitrate, and varying concentrations of zirconyl (IV) nitrate hydrate and cerium (III) nitrate hexahydrate. All experiments were carried at room temperature of $23 \pm 1\ ^{o}C$. Table 1 lists the different compositions of the electrolyte used. The pH was maintained at 1.5 ± 0.1 at the start of each experiment. The deposited powders were scraped from the electrode, dried in a desiccator at room temperature and analyzed.

2.2. Solid State Analyses

The chemical composition of the deposits were measured by energy dispersive x-ray fluorescence spectroscopy (EDXRF) calibrated with bulk samples of ceria and zirconia. The composition was determined over a large region of pressed sorbent powder to verify uniformity of the ceria-zirconia mixture. Four to five measurements were averaged for each sample. Once the powder concentration was found in the desired range of 15-50 mol % zirconia, further analysis by x-ray diffraction (XRD) and transmission

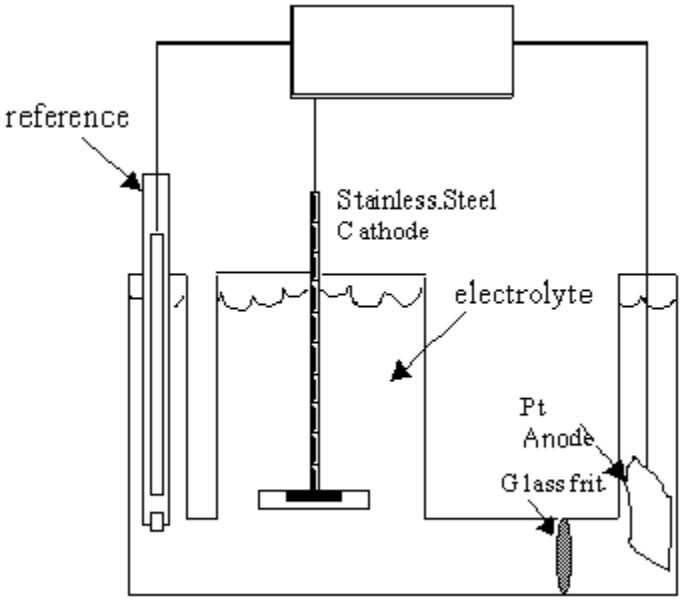

Figure 1. Electrochemical Cell Schematic

Table 1. Composition of the Various Electrolyte Solutions.

Electrolyte	$Ce(NO_3)_3.6H_2O$	$Zr(NO_3)_4.H_2O$	NH_4NO_3 (M)
A	0.5	0.0	0.5
B	0.5	0.1	0.5
C	0.5	0.2	0.5
D	0.25	0.2	0.5
E	0.125	0.2	0.5
F	0.25	0.5	0.5
G	0.125	0.5	0.5

electron microscopy (TEM) were carried out to verify the structure of the material. The crystallinity and particle size of the as produced powder was analyzed by a bright-field high resolution TEM. The phase identification of the sample and the lattice parameters were determined with x-ray diffraction analysis (XRD). Intensity data were collected at ambient temperature in the 2θ range between 25° and 60°, and the peaks of each compound were compared with phases in the International Center for Diffraction Data database (ICDD).

2.2.1. Composition

Figure 2 shows that the final powder composition is a linear function of the initial electrolyte concentration at various applied potentials. At low Zr concentrations in the electrolyte ceria is preferentially deposited over zirconia, which diminishes as the Zr

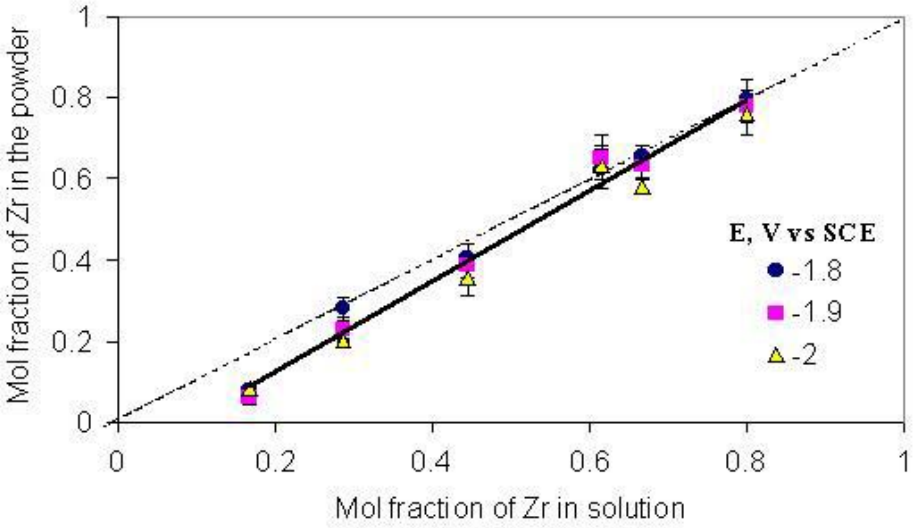

Figure 2. Electrolyte Concentration vs. Final Powder Composition.

concentration of the solution increases. The powder composition was independent of the applied potential. As a reference point, a dashed line has been added to Figure 2 to show the 1:1 correspondence between the mol fraction of Zr in the powder with concentration in solution.

2.2.2. XRD and TEM Characterization

Figure 3 shows high-resolution TEM images of the CeO_2 and CeO_2-ZrO_2 samples. The average grain diameters of the nanocrystallites were approximately 5 nm, independent of composition. Crystallite size of this order compares favorably with many of the standard wet and dry processing production methods. Selected-area electron diffraction (SAED) patterns indicated a crystalline material and suggested the presence of a solid solution.

The crystallite size and phase were also verified with X-ray diffraction (XRD). The XRD of the powder sample having 18 at % Zr is shown in Figure 4 (a) and compared to the standard library patterns of cubic CeO_2 (b) and monoclinic and tetragonal ZrO_2 (c). The spectrum exhibits a cubic single phase similar to solid solution ZrO_2-CeO_2 XRD patterns of samples generated by non-electrochemical techniques. The mean crystal size, calculated from the full width at half maximum of the (111) reflection, was 4.5 nm, which is consistent with the TEM observation. As the concentration of ZrO_2 increased a second phase corresponding to ZrO_2 began to emerge. Formation of a separate ZrO_2 phase is thought to be undesirable for a desulfurization sorbent.

The solid solution must be stable at high temperature if the material is to serve as a good sorbent. The XRD patterns of a sample containing 18.7 mol % ZrO_2 heat treated at 700^{o}C for varying times are shown in Figure 5. Heat treatment was carried out for a

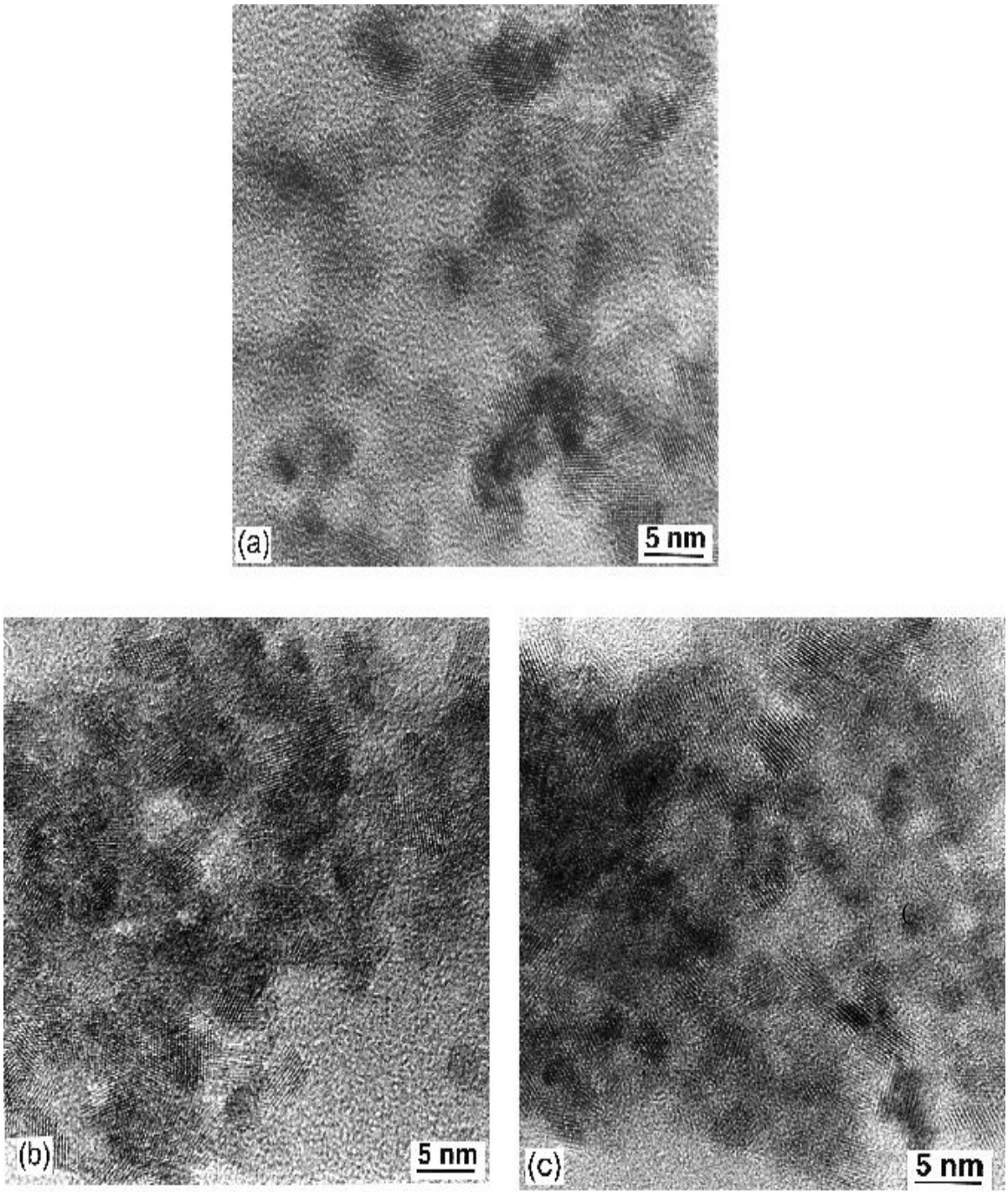

Figure 3. TEM image of (a) Ceria, (b) Ceria-7 at.% Zirconia (C) Ceria-18 at.% Zirconia

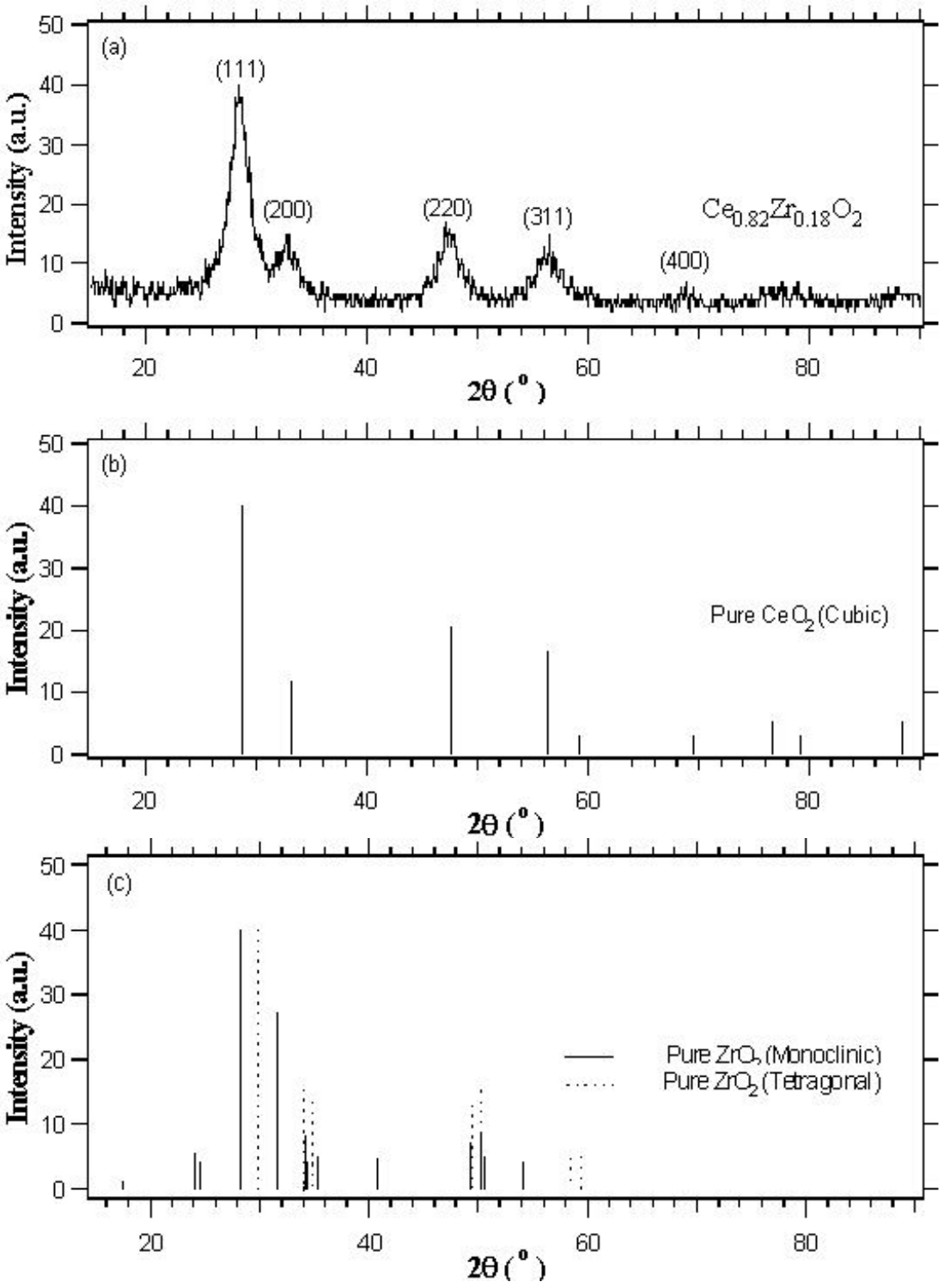

Figure 4. XRD Analysis of (a) Electrochemically Generated Nanocrystalline $Ce_{0.82}Zr_{0.18}O_2$, (b) Cubic CeO_2 (JCPDS 34-394), and (c) Monoclinic (JCPDS 37-1484) and Tetragonal (JCPDS 42-1164) ZrO_2

specified time on a single sample, which was then cooled to room temperature and subjected to XRD analysis. The procedure was repeated with the following heating times: 2, 2, 3, 5, 10, 24, 60 hr (cumulative time of 106 hr). The Al peak in Figure 5 came from the sample holder and was not part of the powder. No phase separation was observed.

The particle size increased slightly with prolonged heat treatment steps, and after 106 hours of heating at 700^0C, the crystallite size was 14.5 nm. Large increases in crystallite size are not considered desirable, but the increase observed here is small enough that it is not considered critical for sorbent performance. A TEM micrograph following heat treatment for 106 hours, verified the increase in crystallite size observed with XRD.

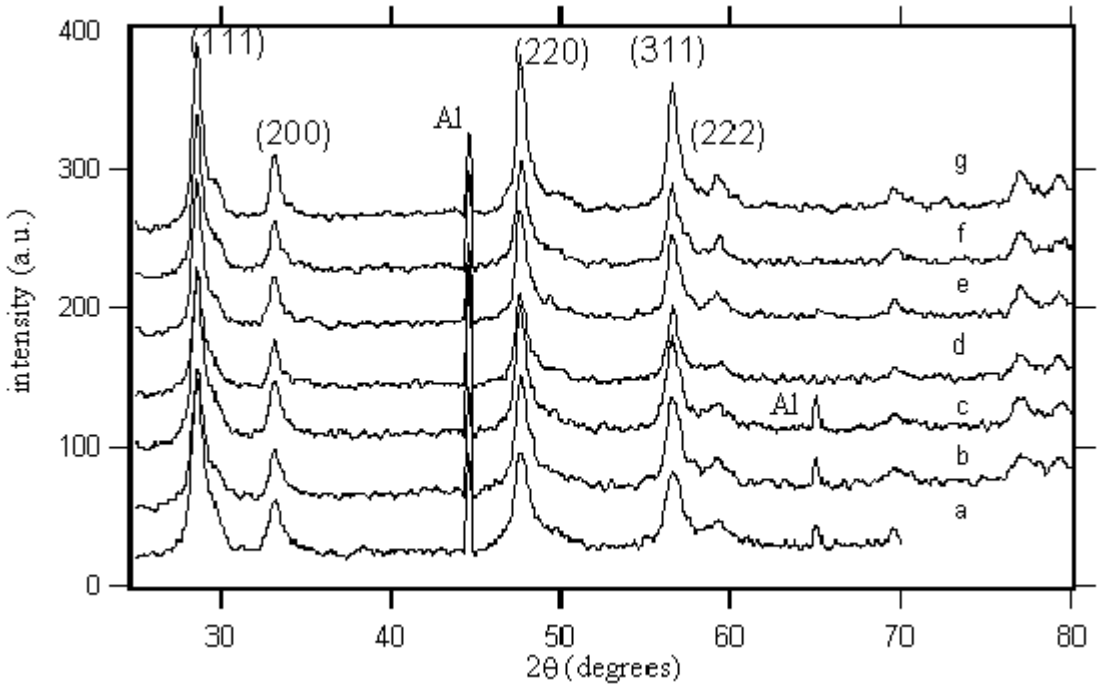

Figure 5. Heat Treated 700°C, 18.7 mol % Zr Ceria-Zirconia with Resulting Crystallite Size of (a) 9.5 nm, (b) 10 nm, (c) 11 nm, (d) 12 nm, (e) 12.5 nm, (f) 12.5 nm, and (g) 14.5 nm.

3. HIGH TEMPERATURE DESULFURIZATION

3.1. Fixed-Bed Reactor

Sorbent performance during H_2S removal is evaluated using the fixed-bed reactor system shown in Figure 6. Gases – H_2S, H_2, N_2, and CO_2 – are obtained from high purity cylinders and flow rates are controlled using calibrated mass flow controllers. The proportions of H_2 and CO_2 in the feed gas can be adjusted to control the reducing power (oxygen partial pressure) of the feed gas. Valves are arranged so that either feed or product gas can be fed to the gas chromatograph for analysis. In addition, N_2 feed gas can be directed past a calibrated H_2S permeation tube where a standard quantity of H_2S is

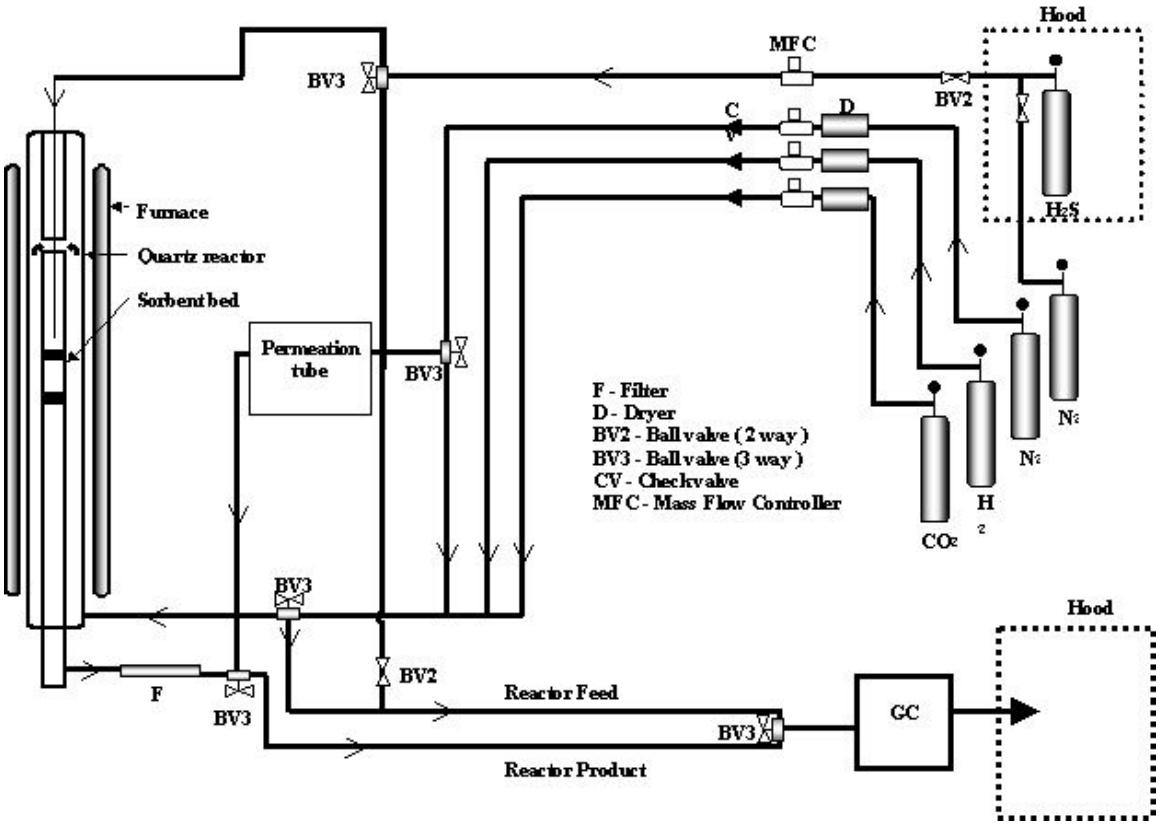

Figure 6. Fixed-Bed Reactor System

added for calibration of the gas chromatograph at low H_2S concentrations (< 10 ppmv). Calibration at higher H_2S concentrations is accomplished by mixing pure cylinder gases using the mass flow controllers.

In normal operation H_2, CO_2, and N_2 are mixed in the desired proportions and fed to the bottom of the quartz reaction vessel. These gases are preheated as they flow upward in the annular region outside of the reactor insert. H_2S is added to the preheated gases just before they contact the sorbent bed, which is supported inside the reactor on a porous quartz disc and quartz wool. Sorbent pre-reduction, if used, is carried out in the same manner except that H_2S is not added. Product gas exits from the bottom of the reactor, and flows through a quartz wool filter to remove any particulate matter and/or traces of elemental sulfur that may be present, and to the gas chromatograph for analysis.

All components of the reactor vessel and insert and all valves are of quartz or Teflon to prevent interaction between low concentrations of H_2S and steel surfaces. Steel surfaces within the gas chromatograph are silcosteel to eliminate interaction. The only untreated steel surfaces that contact H_2S are the feed gas lines.

A more detailed diagram of the reactor, including dimensions, is shown in Figure 7. The total capacity of the reactor is approximately 15 g of solid.

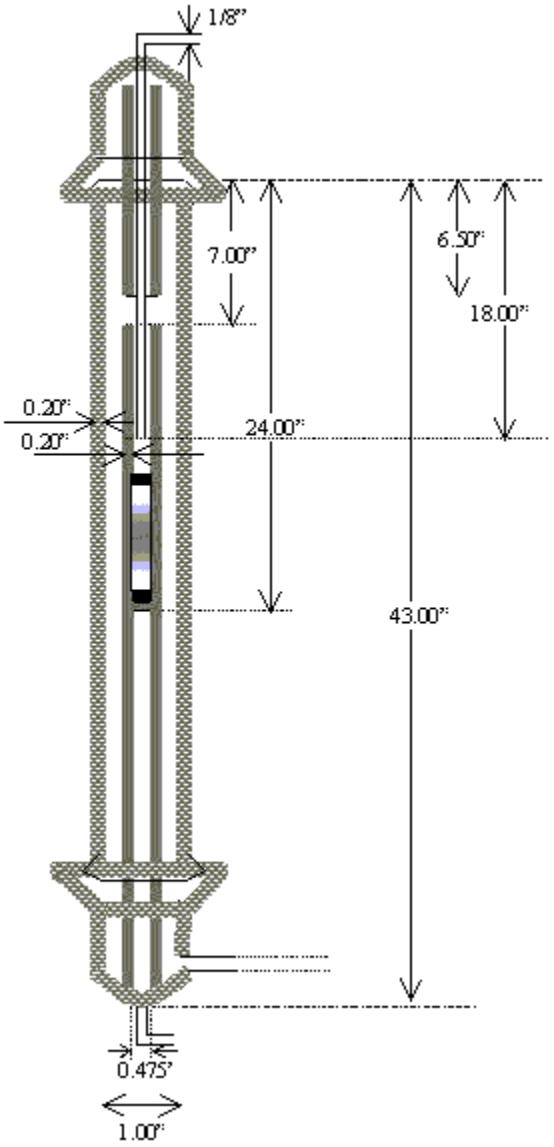

Figure 7. Details of the Quartz Reactor

3.2. Gas Analysis

H_2S concentration of the feed and product gas is determined using a Varian model 3800 gas chromatograph purchased for this project using LSU matching funds. The chromatograph is equipped with dual columns, two Valco multiport sampling valves, and both a pulsed flame photometric detector (PFPD) and a thermal conductivity detector (TCD). The PFPD is used for H_2S concentrations from sub-ppmv to about 10 ppmv, while the TCD is used for concentrations in excess of 100 ppmv. There is a gap in the analytical capability between about 10 and 100 ppmv, but primary interest is in the low concentration range. The PFPD provides analytical capability to approximately 0.1 ppmv

H_2S (100 ppbv) and is about 10 times more sensitive than a standard flame photometric detector.

A summary of chromatograph operating conditions is presented in Table 2.

Table 2. Gas Chromatograph Operating Conditions

PFPD	Column:	CP SIL5, 5 μ
		L = 3 m, D = 530 μ, T = 200°C
	Carrier Gas:	He, 2.9 ml/min
	Sample Loop:	SilcoSteel, 50 μL
TCD	Column:	HAYESEP A SilcoSteel
		L = 3.3 m, D = 3.13 μ, T = 200°C
	Carrier Gas:	He, 28 ml/min
		He, 31.2 ml/min (backflush)
	Sample Loop:	SilcoSteel, 2 ml

The flow arrangement through the two automatic valves (one 10-port and one 6-port) is shown in Figure 8. The upper left diagram shows gas flows in normal operation. The gas to be analyzed enters the 10-port valve at position 4, exits to the PFPD sample loop at position 5, re-enters the 10-port valve at position 8, exits to the TCD sample loop at position 9, again enters the 10-port valve at position 2 and is vented to a laboratory hood through position 3. In this operation mode the contents of both sample loops are continually purged and replenished with the most recent product gas. Three carrier gases are used. Carrier 1 enters the 10-port valve at position 7 and exits at position 6 to the PFPD column and then to the PFPD. Carrier 2 enters the 10-port valve at position 10, exits at position 1, and flows to the 6-port valve. It enters the 6-port valve at position 2 and exits through position 1 to the TCD column, then back into the 6-port valve at position 3 and out through position 4 to the TCD and laboratory vent. Carrier 3 enters the 6-port valve at position 5 and exits through position 6 to vent.

Samples for both the PFPD and TCD are acquired simultaneously by switching the 10-port valve to the position shown in the upper right diagram of Figure 8. The product gas sample enters the 10-port valve at position 4 and exits through position 3 directly to the laboratory vent. Carrier gas 1 enters the 10-port valve at position 7, exits through position 8 and picks up the sample from the PFPD sample loop. It reenters the 10-port valve at position 5 and exits through position 6 to the PFPD column. Column effluent then flows directly to the PFPD. Carrier gas 2 enters at position 10 and exits through position 9 where it picks up the TCD sample. It re-enters the 10-port valve at position 2 and exits through position 1 to the 6-port valve. The TCD sample enters the 6-port valve at position 2 and exits to the TCD column through position 1. The TCD column effluent re-enters the 6-port valve at position 3 and exits through position 4 to the TCD. Flow of carrier 3 is unchanged. It enters the 6-port valve at position 5 and exits through position 6 to vent.

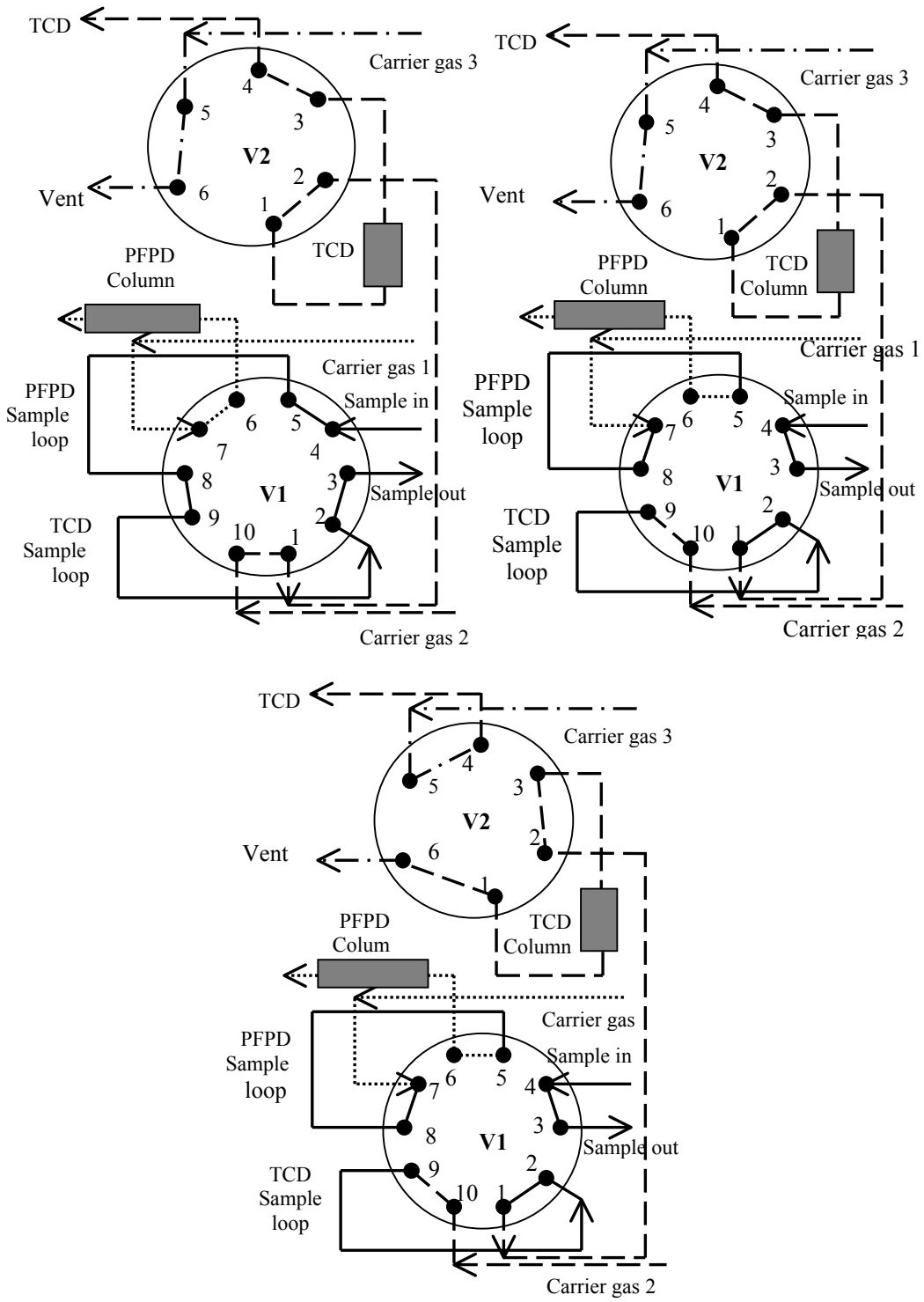

Figure 8. Chromatograph Sampling Arrangement

The position of the 6-port valve is switched in the lower center diagram of Figure 8 to permit H_2O formed during the desulfurization reaction to be backflushed to vent. Switching occurs after H_2S has been eluted from the TCD column but before water is eluted. Sample gas and carrier gas 1 flows are not changed from the previous case. However, with the 6-port valve in the new position, carrier gas 2 flows through the 10-port valve as before. It enters the 6-port valve at position 2, exits through position 3, and flows in the reverse direction through the TCD column to backflush the H_2O. Carrier gas 2 plus the H_2O then re-enters the 6-port valve at position 1 and exits through position 6 directly to vent. Carrier gas 3 enters the 6-port valve at position 5 and exits through position 4 to the TCD so that carrier gas flow is maintained through the TCD at all time.

PFPD calibration was accomplished by flowing N_2 at a known rate past a calibrated H_2S permeation tube maintained at 30^oC (see Figure 6). A PFPD calibration curve between 0.1 and 6 ppmv H_2S is shown in Figure 9. The chromatogram obtained from the 0.1 ppmv H_2S sample shown in Figure 10 indicates that the signal-to-noise ratio is strong even at this low H_2S concentration. The best calibration was obtained by correlating H_2S peak height versus H_2S concentration using a third order polynomial with a zero intercept. The calibration equation shown on the figure has a R^2 value of 0.9982.

TCD calibration was accomplished by mixing N_2 and H_2S from the high purity cylinders with flow rates controlled using the mass flow controllers. Results of the TCD calibration between 100 ppmv and 1.5% (15,000 ppmv) are shown in Figure 11. The calibration was also based on H_2S peak height using a second order polynomial with a zero intercept and the R^2 value was 0.9996.

Calibration curves are checked periodically and the detectors are recalibrated when necessary.

3.3. Materials

Because it was impossible to produce sufficient quantities of CeO_2 and CeO_2-ZrO_2 needed for desulfurization testing using electrochemical synthesis a number of sorbent materials from other sources have been acquired and screened for desulfurization performance. The screening indicated that sorbents having similar properties would be required if the effects of ZrO_2 addition were to be evaluated. Test materials have been acquired from Rhone Poulenc, NexTech Materials, Alfa Aesar and have been synthesized in the LSU laboratory using a coprecipitation technique. Because of the need for the sorbents to have similar properties, we are now concentrating on materials synthesized at LSU. These materials are being characterized in terms of their x-ray diffraction patterns, specific surface area, and reducibility in addition to their ability as a H_2S sorbent.

3.3.1 Sorbents Acquired from Other Sources

A total of six CeO_2 and CeO_2-ZrO_2 compounds obtained from Rhone Poulenc, Alfa Aesar, and NexTech Materials have been acquired and subjected to selected

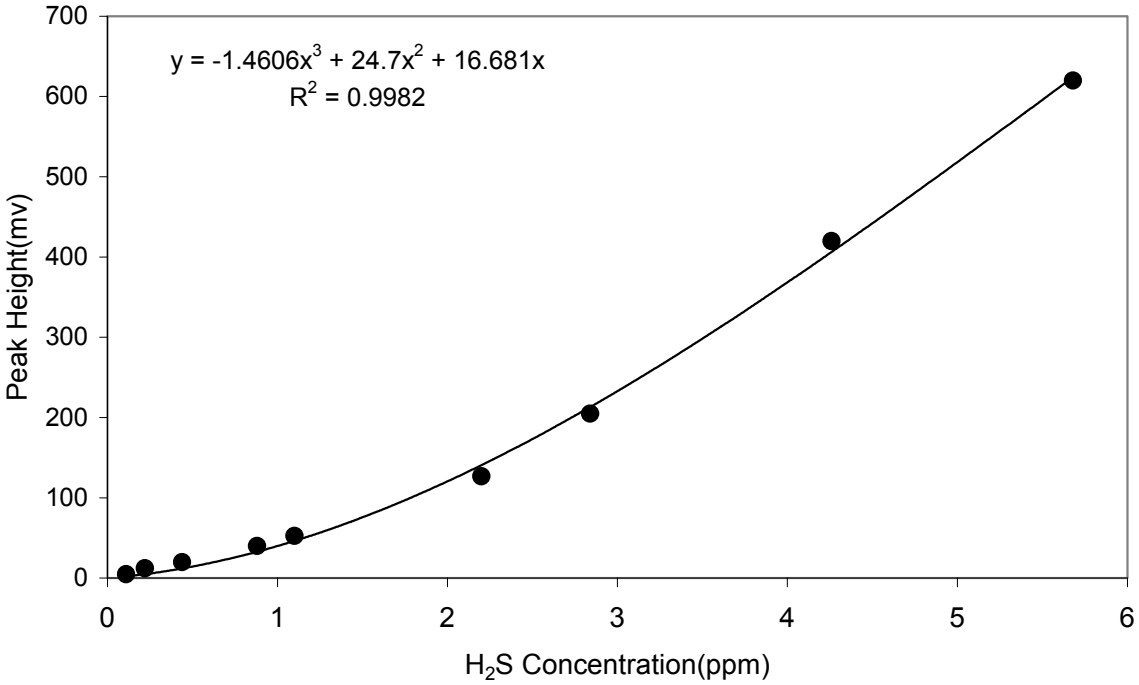

Figure 9. PFPD Calibration Curve

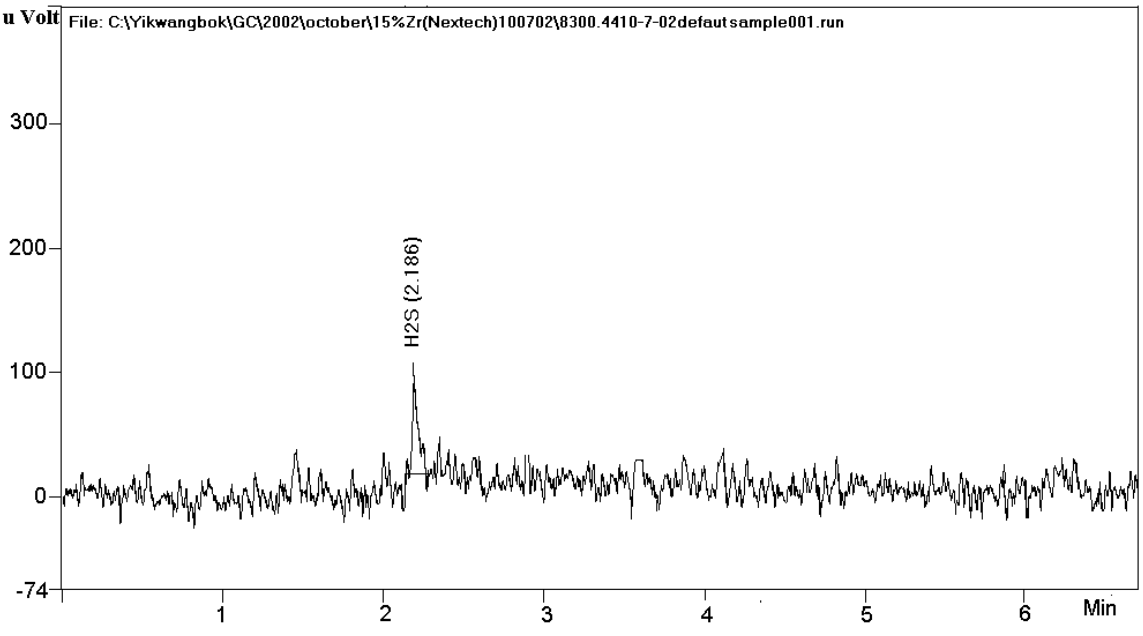

Figure 10. PFPD Chromatogram at 0.01 ppmv H_2S

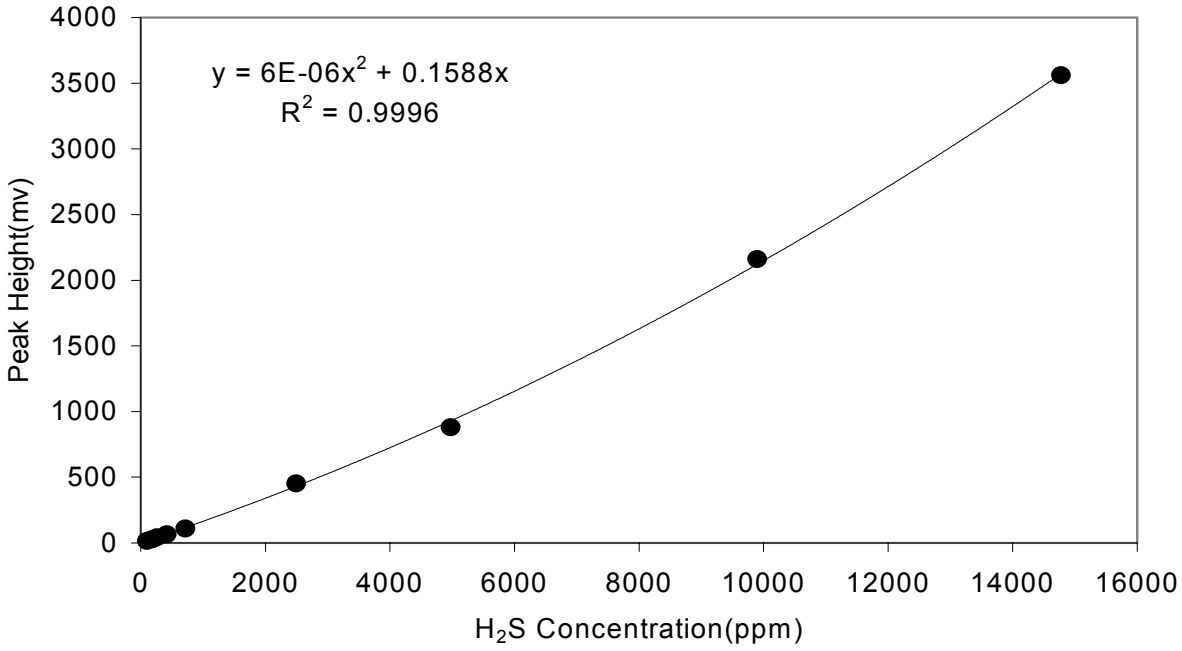

Figure 11. TCD Calibration Curve

characterization and desulfurization tests. A list of these compounds with selected properties is presented in Table 4. Surface areas of the as-received materials were either measured at LSU or reported by the manufacturer, while all surface areas following calcination were determined at LSU. Crystallite sizes were determined at LSU based on line broadening analysis of the 111 XRD peak. Note that characterization has not been completed at this time.

The CeO_2 from Rhone Poulenc is the same material used in the earlier studies at LSU (Zeng et al. 1999 and Zeng et al. 2000). The as received material is considered to be 91% CeO_2 since it experiences a 9% weight loss when heated to high temperature in an inert gas. The surface area of the as-received material is based on data from Zeng while crystallite size and surface area following calcination were measured in this project.

Properties of the CeO_2 and $Ce_2(CO_3)\cdot xH_2O$ from Alfa Aesar were determined at LSU. The purity of the CeO_2 was 99.5%. Upon calcination, the $Ce_2(CO_3)_3\cdot xH_2O$ should decompose to CeO_2. We were interested in this compound as a possible sorbent precursor because of the possibility that the calcined material would have an extremely large surface area and therefore be extremely reactive. As shown in Table 3, the high surface area did not develop.

Table 3. CeO_2 and CeO_2-ZrO_2 Materials and Selected Properties

Compound/Source	Surface Area, m^2/g		Crystallite Size, nm
	As-Received	Calcined*	
CeO_2/Rhone Poulenc	156	110	2.5
CeO_2/Alfa Aesar	47.8	45.8	25
$Ce_2(CO_3)_3 \cdot xH_2O$/Alfa Aesar	48.7	39.9	NA
85%CeO_2-15%ZrO_2/NexTech	109	80	9.4
80%CeO_2-20%ZrO_2/NexTech	144	NA	8.7
70%CeO_2-30%ZrO_2/NexTech	124	67	NA

* at 700°C for 4 hr in N_2 NA not available

Approximately 50g each of three CeO_2-ZrO_2 samples were donated by NexTech Materials for the project. These amounts were sufficient for characterization, but not for complete desulfurization testing where between 1.5 and 6 g of sorbent is required for each test. The x-ray diffraction spectrum of the NexTech material containing 80%CeO_2-20%ZrO_2 presented in Figure 12 shows no significant difference from the spectrum of the 78%CeO_2-18%ZrO_2 material prepared electrochemically at LSU and shown in Figure 5. The most important result is that there is no indication of a separate ZrO_2 phase in either of the spectra.

Only the Alfa Aesar products were available in the quantities needed for desulfurization testing and, as shown in Table 4, their surface areas were considerably smaller and crystallite sizes considerably larger than the other materials. In addition, only one CeO_2-ZrO_2 composition was available from Alfa Aesar. Because of these limitations we began to prepare CeO_2 and CeO_2-ZrO_2 compounds at LSU. These materials are described in the following section.

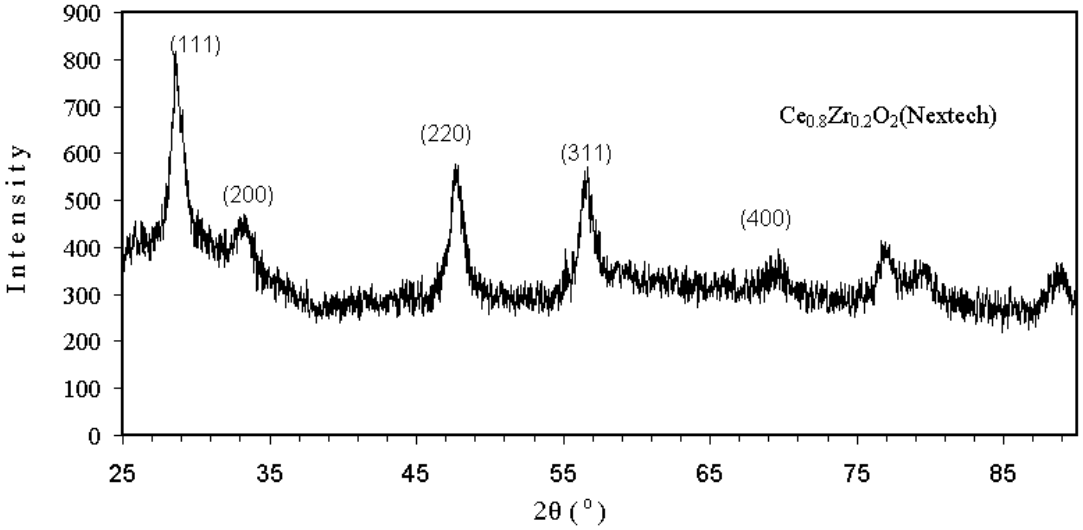

Figure 12. XRD Spectrum for 80%CeO_2-20%ZrO_2 Material from NexTech

3.3.2. Sorbents Prepared at LSU

CeO_2 and three CeO_2-ZrO_2 compounds have been prepared using the coprecipitation technique described by Rossignol et al. (1999). An aqueous solution containing desired proportions of cerium (III) nitrate hexahydrate and zirconyl nitrate hydrate was prepared. The mixture was held at 50°C for 30 minutes to insure complete solution. Precipitation was induced by slowly adding an excess of 25% NH_4OH solution. The temperature was then raised to 100°C where the liquid slowly evaporated over a period of about 4 to 5 hours. The dried powder was then calcined at 400°C for 2 hours. The calcined product was then crushed and sieved with the 150 – 300 μm fraction retained for testing.

Properties of these materials, which are summarized in Table 4, are between those of the Alfa Aesar and NexTech materials. Since the properties also appear to be reasonably independent of composition, we have begun desulfurization tests to evaluate the effect of ZrO_2 addition.

Table 4. CeO_2 and CeO_2-ZrO_2 Materials Prepared at LSU by Coprecipitation

Compound	Surface Area, m^2/g		Crystallite Size, nm
	As-Received	Calcined*	
CeO_2	58.5	NA	21.7
95%CeO_2-5%ZrO_2	NA	NA	19.1
90%CeO_2-10%ZrO_2	NA	NA	NA
80%CeO_2-20%ZrO_2	76.9	55.8	16.6

* at 700°C for 4 hrs in N_2 NA not available

XRD spectra for the pure CeO_2 and 80%CeO_2-20%ZrO_2 materials prepared at LSU are compared in Figure 13. The two spectra are essentially identical and there is no indication of a separate ZrO_2 phase. In addition, these spectra are also effectively identical to those shown in Figures 5 and 11.

3.4. Sorbent Reduction

The ability to reduce CeO_2 to CeO_n ($1.5 < n < 2.0$) has been studied using an electrobalance reactor. In these tests the sorbent was initially exposed to an inert atmosphere and heated to 800°C until the weight became constant. The sample was then cooled and subsequently heated slowly in a reducing atmosphere to 1000°C. Weight loss in the reducing atmosphere is directly related to the value of n in CeO_n. Selected sorbents have been tested using three different reducing gas compositions:

Gas 1	10% H_2, 0.0% CO_2, balance He
Gas 2	10% H_2, 3.5% CO_2, balance He
Gas 3	50% H_2, 3.5% CO_2, balance He.

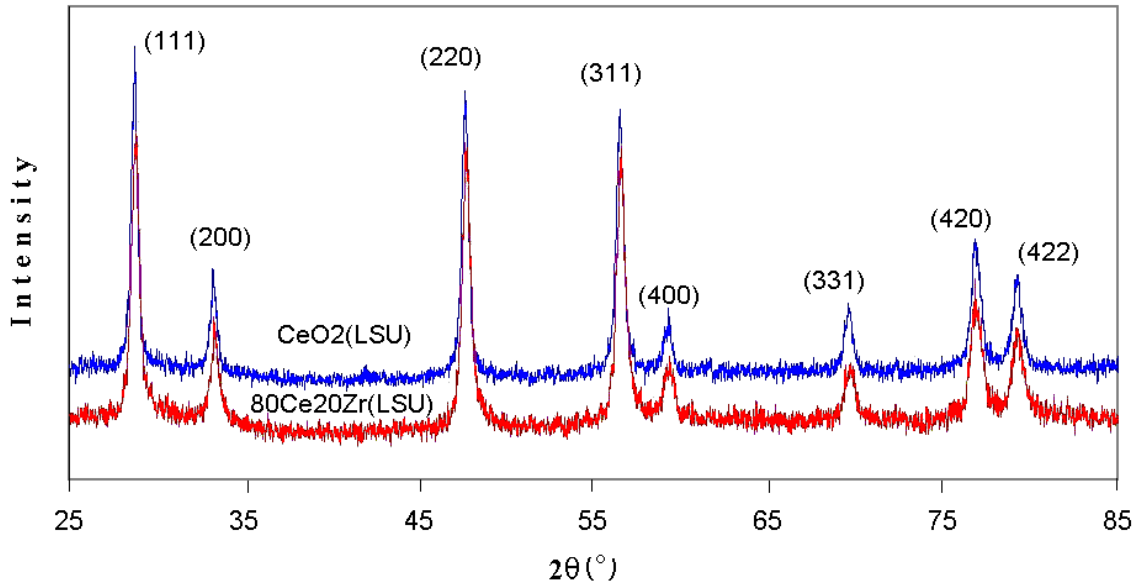

Figure 13. XRD Spectrum for 80%CeO_2-20%ZrO_2 Material from LSU and CeO_2 Material from LSU

The equilibrium partial pressure of O_2 provides a measure of the reducing power of the gas. Gas 1 is oxygen free except for trace impurities present in the H_2 and He, and has, in principle, the greatest reducing power. The presence of CO_2 in the other gases provides small quantities of free O_2 at elevated temperatures and the ratio of H_2 to CO_2 determines the amount of free O_2 and the reducing power. Results of equilibrium partial pressure calculations for Gases 2 and 3 as a function of temperature, performed using HSC Chemistry, are shown in Figure 14. The equilibrium O_2 pressure ranges from about 10^{-32} atm at 400°C to 10^{-14} atm at 1000°C, with the equilibrium O_2 pressure being 1 to 2 orders of magnitude lower in reducing Gas 3. At 700°C, the most common experimental desulfurization temperature in the experiments completed to date, the equilibrium O_2 pressures are about 10^{-21} and 10^{-20} atm for Gases 3 and 2, respectively.

Reduction results in the three reducing gases using Rhone Poulenc CeO_2 are compared in Figure 15 where the value of n in CeO_n is plotted as a function of temperature. In Gas 1 (most highly reducing) reduction began at about 650°C and the value of n at the final 1000°C temperature was 1.81. In Gas 3 having intermediate reducing power reduction began near 700°C and the final value of n was 1.85. In the least reducing Gas 2 reduction also began at about 700°C and the final value of n was 1.88. The difference in the level of reduction in Gases 2 and 3 became appreciable at about 750°C. These values of n are in reasonable agreement with experimental values published by Bevan and Kordis (1964) based on the O_2 pressures of Figure 14.

Figures 16 and 17 compare the reducibility of Rhone Poulenc CeO_2 with the 80% CeO_2-20% ZrO_2 material produced at LSU by coprecipitation. Figure 16 is based on

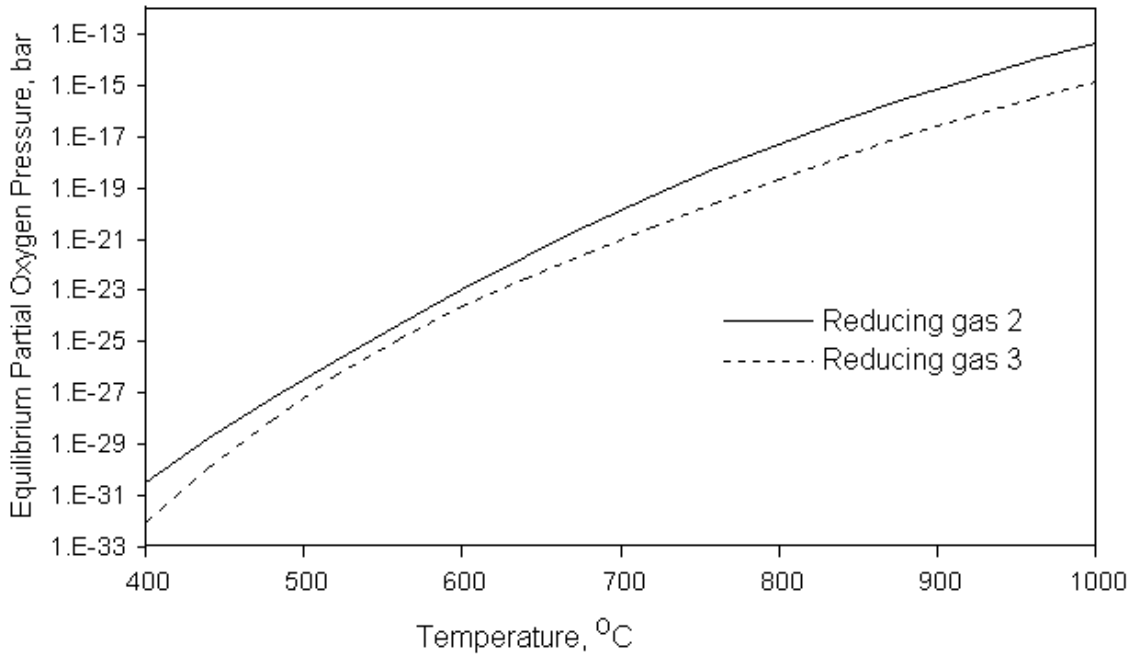

Figure 14. Equilibrium Oxygen Pressure in Reducing Gases 2 and 3.

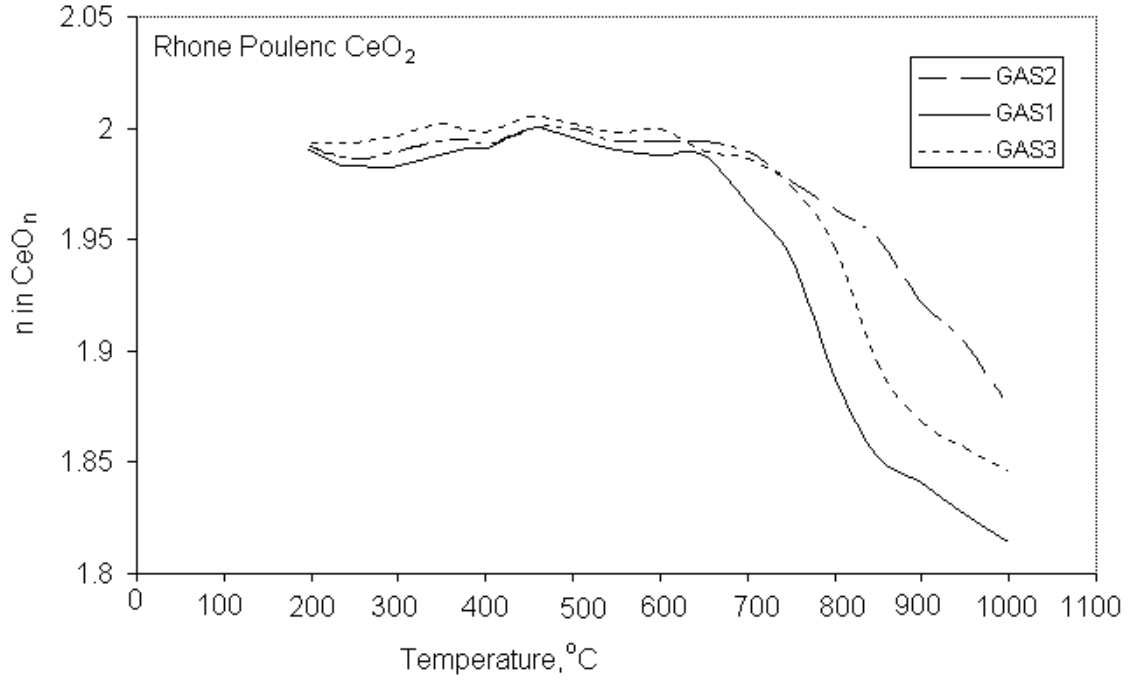

Figure 15. Reduction of Rhone Poulenc CeO_2

results using Gas 1 (most highly reducing) while Figure 17 presents data in Gas 2 (least reducing). The electrobalance response curves appear somewhat variable because of the extremely small weight losses associated with reduction. For example, reduction of pure CeO_2 to $CeO_{1.95}$ represents as weight loss of less than 0.5%. In both cases reduction of the CeO_2-ZrO_2 began in the range of 400 to 450 ^oC, compared to an initial reduction temperature of almost 700^oC for pure CeO_2. The final values of n for CeO_2-ZrO_2 were 1.77 and 1.84 in Gases 1 and 2, respectively, compared to 1.82 and 1.88 for Rhone Poulenc CeO_2 in the same atmospheres.

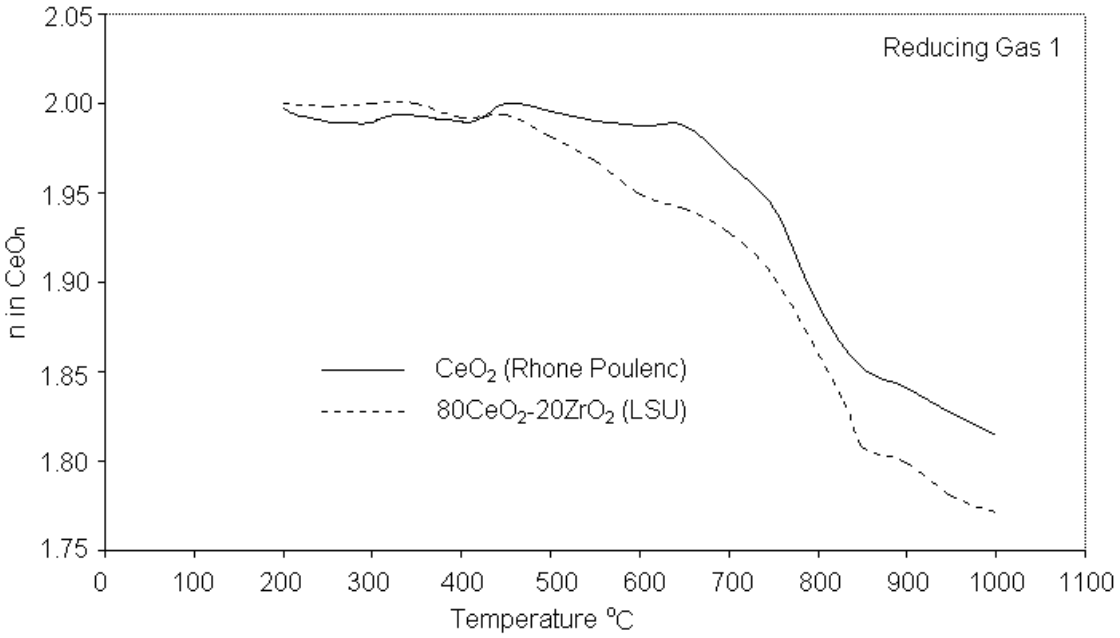

Figure 16. Comparison of Reducibility of CeO_2 (Rhone Poulenc) and 80%CeO_2-20%ZrO_2 (LSU Coprecipitation) in Reducing Gas 1.

The results shown in Figures 15 through 17 are typical of all reduction results as shown by the data summary presented in Table 5. The temperatures corresponding to values of n = 1.98, 1.86, and 1.80 as well as the value of n at the final temperature of 1000^oC are presented for eight test materials using the three reducing gases. Roughly speaking, the temperature corresponding to n = 1.98 represents the beginning of reduction for each sorbent, while the temperature for n = 1.86 is at an intermediate condition of reduction for CeO_2-ZrO_2 sorbents and near the end of reduction of CeO_2 materials. Finally, the temperature for n = 1.76 is near the near of reduction for most of the CeO_2-ZrO_2 sorbents. Reduction results are included for one of the CeO_2-ZrO_2 materials produced at LSU electrochemically as well as for the single 80% CeO_2-20% ZrO_2 LSU sorbent produced by coprecipitation for which reduction testing has been completed.

Table 5 clearly shows that CeO_2 from Alfa Aesar is the most difficult to reduce while the CeO_2-ZrO_2 materials from NexTech are the most easily reduced. Reduction of the NexTech materials begins at about 300^oC and final values of n < 1.7 were achieved

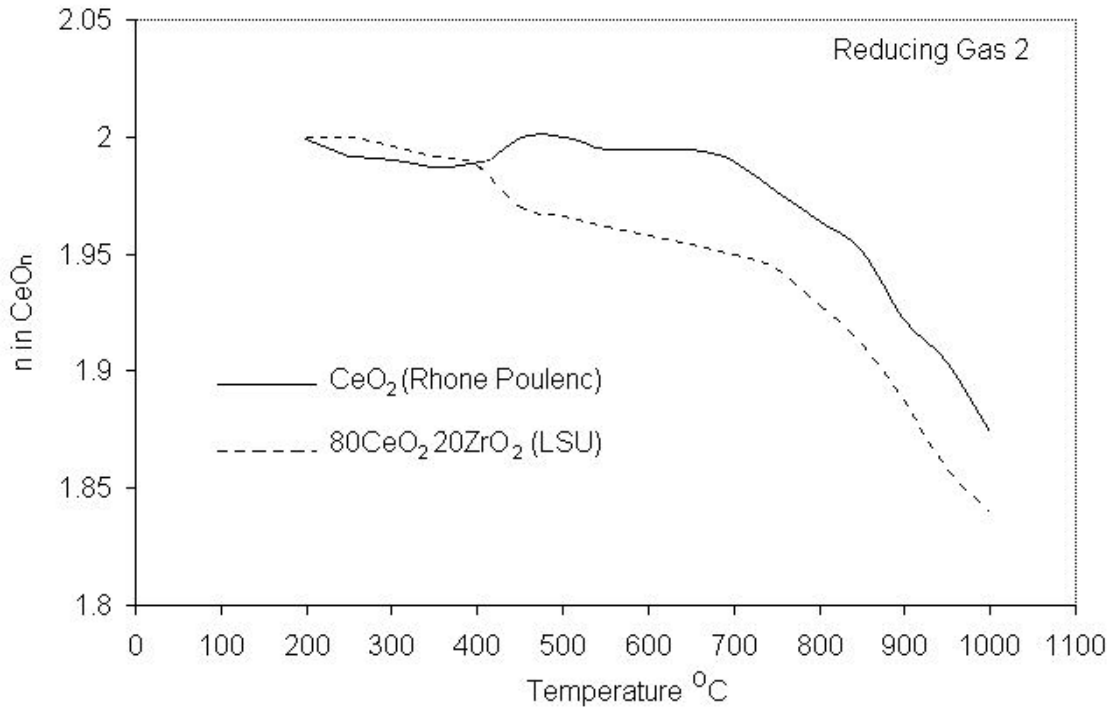

Figure 17. Comparison of Reducibility of CeO_2 (Rhone Poulenc) and 80%CeO_2-20%ZrO_2 (LSU Coprecipitation) in Reducing Gas 2.

for all three NexTech sorbents in the most strongly reducing gas, and in all three gases for the material containing 30% ZrO_2. The LSU materials show intermediate reducibility.

3.5. Fixed-Bed Desulfurization Experiments

The test sorbent, either CeO_2 or CeO_2-ZrO_2, was first pressed into tablets using a hydraulic press at 20,000 psi. The resulting tablets were then crushed and sieved with the 150-300 μm size range used in reaction tests. Sorbent was mixed with Al_2O_3 in a 1-to-2 ratio by weight and a selected amount of the mixture was added to the reactor. Tablets were formed because the small particle size of the as-received sorbent materials produced excessive pressure drop through the reactor, and the Al_2O_3 was added to control sintering. Zeng et al. (1999) found that the sorbent without Al_2O_3 sintered into a loosely bound chalk-like mass after testing. With the added Al_2O_3 the mixture could be removed from the reactor as a free-flowing powder after tests.

A typical breakthrough curve showing H_2S concentration as a function of dimensionless time is shown in Figure 18. Dimensionless time is defined as the ratio of the actual reaction time to the time corresponding to complete conversion of CeO_2 to Ce_2O_2S if 100% of the H_2S fed were removed. For practical purposes during the early stages of the reaction when H_2S removal is almost complete, dimensionless time is also equal to the fractional conversion of CeO_n. This run used 2 g of Rhone Poulenc CeO_2

and 4 g of alumina at a total feed rate of 80 cm^3(stp)/min. Reaction temperature was 700°C and the feed gas contained 89.75% N_2, 10% H_2, and 0.25% H_2S.

Table 5. Summary of Reduction Results for Eight Test Sorbents

Compound/Source	Temperature, °C, Corresponding to Indicated Value of n			Final Value of n at 1000°C
	1.98	1.86	1.80	
Gas 1				
CeO_2/Rhone Poulenc	660	840	---	1.81
CeO_2/Alfa Aesar	670	850	1000	1.80
$Ce_2(CO_3)_3 \cdot xH_2O$/Alfa Aesar	700	880	---	1.82
85%CeO_2-15%ZrO_2/Nextech	280	690	770	1.69
80%CeO_2-20%ZrO_2/Nextech	370	670	760	1.69
70%CeO_2-30%ZrO_2/Nextech	310	530	760	1.65
80%CeO_2-20%ZrO_2/LSU*	420	800	900	1.78
80%CeO_2-20%ZrO_2/LSU**	460	910	---	1.82
Gas 2				
CeO_2/Rhone Poulenc	730	---	---	1.88
CeO_2/Alfa Aesar	830	---	---	1.91
$Ce_2(CO_3)_3 \cdot xH_2O$/Alfa Aesar	860	---	---	1.91
85%CeO_2-15%ZrO_2/NexTech	310	810	980	1.77
80%CeO_2-20%ZrO_2/NexTech	300	775	890	1.78
70%CeO_2-30%ZrO_2/NexTech	305	550	680	1.69
80%CeO_2-20%ZrO_2/LSU*	420	940	---	1.84
80%CeO_2-20%ZrO_2/LSU**	560	970	---	1.86
Gas 3				
CeO_2/Rhone Poulenc	730	930	---	1.85
CeO_2/Alfa Aesar	770	950	---	1.85
$Ce_2(CO_3)_3 \cdot xH_2O$/Alfa Aesar	765	---	---	1.87
85%CeO_2-15%ZrO_2/NexTech	300	720	800	1.74
80%CeO_2-20%ZrO_2/NexTech	275	720	810	1.72
70%CeO_2-30%ZrO_2/NexTech	310	550	680	1.68
80%CeO_2-20%ZrO_2/LSU*	450	820	910	1.78
80%CeO_2-20%ZrO_2/LSU**	470	760	870	1.76

* LSU prepared by coprecipitation ** LSU prepared by electrodeposition

We attribute the small "bump" near the beginning of the reaction to the fact that H_2S initially contacted unreduced or partially reduced CeO_2. However, a reduction reaction front downstream of the sulfidation reaction front soon produced CeO_n with n corresponding to the equilibrium value in a gas closely resembling reducing Gas 1. Once this occurred, H_2S removal was almost complete for t* < ~ 0.9. On the scale shown, the H_2S concentration appears to be effectively zero. Breakthrough began at t* ~ 0.9, and the H_2S concentration gradually increased and approached the inlet concentration at t* ~ 1.2.

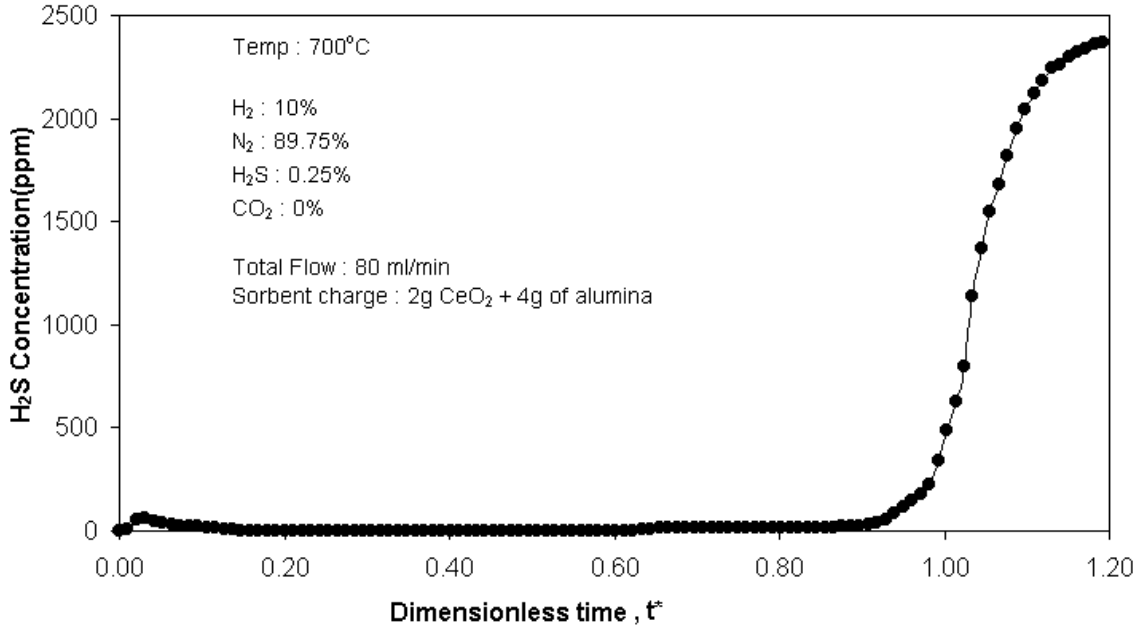

Figure 18. Complete Sulfidation Breakthrough Curve

Figure 19 compares H_2S concentrations versus dimensionless time for tests using CeO_2 and three CeO_2-ZrO_2 mixtures containing 5%, 10%, and 20% ZrO_2 prepared at LSU using the coprecipitation method. Reaction conditions were identical to those shown in Figure 18 for Rhone Poulenc CeO_2, but the tests were terminated at t* ~ 0.8 or 0.9 before full breakthrough could occur. On the scale of Figure 19, prebreakthrough H_2S concentrations were effectively zero for all sorbents for t* < 0.4. Breakthrough began at t* ~ 0.4 for the sorbent containing 20% ZrO_2, at t* ~ 0.45 with 10% ZrO_2, t* ~ 0.5 with 5% ZrO_2, and t* ~ 0.6 for pure CeO_2. While these results suggest that addition of ZrO_2 actually harms desulfurization, a different picture emerges when results are presented using different H_2S concentration and time scales.

Results from the same four tests are presented in Figure 20 for t* ≤ 0.5 and using a greatly expanded H_2S concentration scale from 0 to 6 ppmv. For pure CeO_2 the initial "bump" in H_2S concentration approached 6 ppmv at t* ~ 0.03. Thereafter the H_2S concentration gradually decreased to a value less than 2 ppmv. When 5% ZrO_2 was added, the initial bump maximized at about 3.5 ppmv and the H_2S concentration very

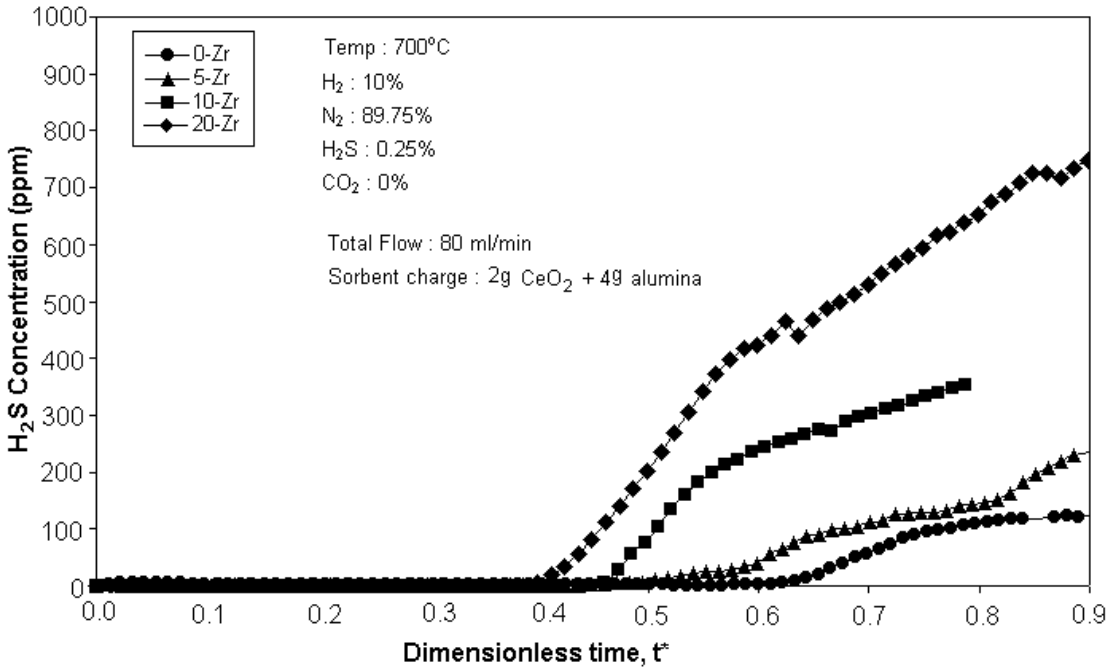

Figure 19. Comparison of H_2S Breakthrough Curves for CeO_2 and CeO_2-ZrO_2 Sorbents Prepared at LSU Using the Coprecipitation Method

quickly decreased to just above 0.1 ppmv. The initial "bump" was absent when the sorbents containing 10% or 20% ZrO_2 were used, and the H_2S concentrations in those tests were below 0.1 ppmv prior to breakthrough. We attribute the decrease and then disappearance of the "bump" to the increased ease at which CeO_2 is reduced in the presence of ZrO_2, and the decreased prebreakthrough H_2S concentrations to the increased equilibrium level of reduction, i.e., to a smaller value of n in CeO_n. Thus, while breakthrough occurs at an earlier time when the sorbent contains ZrO_2, the prebreakthrough H_2S concentration is clearly lower in the presence of ZrO_2, and it is minimum prebreakthrough concentration that is the primary objective of the project.

The importance of structure in determining H_2S removal capability is illustrated in Figure 21 were H_2S concentration is shown as a function of dimensionless time for tests using CeO_2 (no ZrO_2) sorbents from three different sources – from Rhone Poulenc, Alfa Aesar, and prepared at LSU using coprecipitation. These runs were terminated at t* = 0.9. Reaction conditions were the same as described in the previous figures. CeO_2 from Alfa Aesar wass clearly the least reactive with an H_2S maximum of about 140 ppmv followed by a decrease to about 100 ppmv and a very slight increase thereafter. The H_2S maximum using the Rhone Poulenc CeO_2 was about 60 ppmv and the concentration then decreased to less than 1 ppmv and remained at that level until t* = 0.55. The minimum H_2S "bump" occurred with the LSU CeO_2 at about 6 ppmv and the concentration was about 0.1 ppmv until breakthrough began at about t* = 0.55 (as shown in Figure 20).

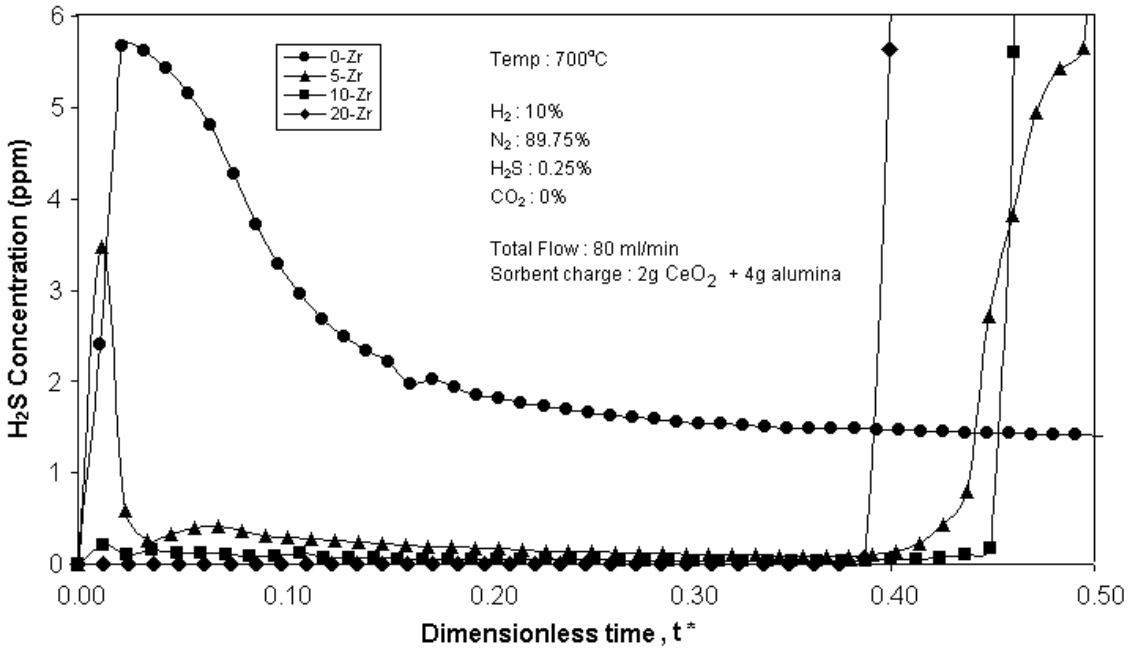

Figure 20. Comparison of H_2S Breakthrough Curves for CeO_2 and CeO_2-ZrO_2 Sorbents Prepared at LSU Using the Coprecipitation Method (Low H_2S Concentrations)

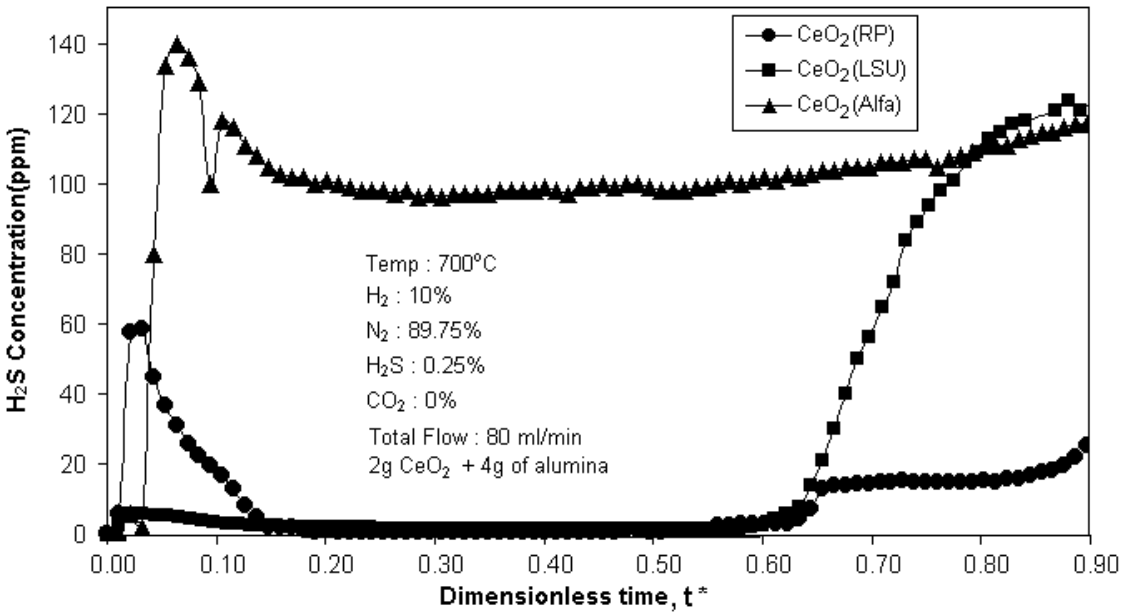

Figure 21. Comparison of H_2S Breakthrough Curves Using CeO_2 Sorbents from Three Sources

4. CONCLUSIONS

The electrochemical production of CeO_2-ZrO_2 powders with nanometric crystallites has been demonstrated for the first time. The XRD and TEM properties of the electrosynthesized CeO_2-ZrO_2 confirmed the existence of a solid solution of ZrO_2 in CeO_2 at Ce to Zr ratios of interest. A separate ZrO_2 phase could be identified only at quite high concentrations of ZrO_2. Unfortunately, the quantities of sorbent produced electrochemically were not sufficient to carry out a desulfurization test program. Hence, CeO_2 and CeO_2-ZrO_2 materials from a number of other sources were considered.

The structural characteristics, reducibility, and desulfurization ability of CeO_2 and CeO_2-ZrO_2 have been investigated. The XRD spectra of all materials showed the existence of a solid solution of ZrO_2 in CeO_2. Reduction tests using an electrobalance reactor have confirmed that addition of ZrO_2 permits reduction to begin at a lower temperature and allows greater reduction of CeO_2 to CeO_n, i.e., produces smaller values of n at equilibrium. Preliminary desulfurization tests indicated that sorbents having similar structural properties would be required to evaluate the effect of ZrO_2 additions. For this reason an in-house coprecipitation procedure for the production of CeO_2 and CeO_2-ZrO_2 mixtures having similar properties has been developed.

Desulfurization testing to date has been limited to a temperature of 700^oC using highly reducing feed gases. Prebreakthrough H_2S concentrations in these tests have decreased at the ZrO_2 level increased, and levels near 0.1 ppmv have been achieved using sorbent compositions of 90% CeO_2-10% ZrO_2 and 80% CeO_2-20% ZrO_2. The primary objective for the remainder of the study is to determine if similarly low prebreakthrough concentrations can be achieved at other temperatures and using feed compositions more representative of gases produced from commercial coal gasification processes.

5.0. REFERENCES

Bevan, D. and Kordis, J., 1964, Mixed Oxides of the Type MoO_3 – 1. Oxygen Dissociation Pressure and Phase Relationship in the System CeO_2-Ce_2O_3 at High Temperatures, Journal of Inorganic and Nuclear Chemistry, 26, 1509.

Bunluesin, T., Gorte, R., and Graham, G., 1997, CO Oxidation for the Characterization of Reproducibility in Oxygen Storage Components of Three-Way Automotive Catalysts, Applied Catalysis B., Environmental, 14, 105.

Cuif, J.-P., Blanchard, G., Touret, O., Marczi, M., and Quemere, E., 1996, Proceedings of the 1996 International Fall Fuels and Lubricants Meeting of the Society of Automotive Engineers, San Antonio, TX, 73.

Focht, G. D., Ranade, P. V., and Harrison, D. P., 1988, High Temperature Desulfurization Using Zinc Ferrite: Reduction and Sulfidation Kinetics, Chemical Engineering Science, 43, 3005.

Gibson, J. B., and Harrison, D. P., 1980, The Reaction Between Hydrogen Sulfide and Single Spherical Pellets of Zinc Oxide, Industrial and Engineering Chemistry, Process Design and Development, 19, 231.

Harrison, D. P., 1998, Performance Analysis of ZnO-Based Sorbents in Removal of H_2S from Fuel Gas, in Desulfurization of Hot Coal gas, A. Atimtay and D. P. Harrison, eds., Springer, Berlin, 213.

Hori, C., Permana, H., Ng, K., Brenner, A., Moore, K., Rahmoeller, K., and Belton, D., 1998, Thermal Stability of Oxygen Storage Properties in a Mixed CeO_2-ZrO_2 System, Applied Catalysis B, Environmental, 16, 105.

Mukherjee, A., Yi, K., Podlaha, E., and Harrison, 2001, High Efficiency Desulfurization of Synthesis Gas, Annual Report, U.S Department of Energy Project DE-PS26-00FT40676.

Ozawa, M., 1997, Role of Cerium-Zirconium Mixed Oxides as Catalysts for Car Pollution: A Short Review, Journal of Alloys and Compounds, 275, 886.

Podlaha, E. P., Bogli, A., Bonhote, Ch., and Landolt, D., 1997, Development of a New, Pseudo-Inverted Disk Electrode, Journal of Applied Electrochemistry, 27, 805.

Rossignol, S., et al., 1999, Preparation of Zirconia-Ceria Materials by Soft Chemistry, Catalysis Today, 50, 261.

Sorensen, O., 1976, Thermodynamic Studies of the Phase Relationships of Nonstoichiometric Cerium Oxides at Higher Temperatures, Journal of Solid State Chemistry, 18, 217.

Switzer, A., 1987, Electrochemical Synthesis of Ceramic Films and Powders, Journal of the American Ceramic Society Bulletin, 66[10], 1521.

Trovarelli, A., 1996, Catalytic Properties of Ceria and CeO_2-Containing Materials, Catalysis Reviews: Science and Engineering, 38, 439.

Trovarelli, A., de Leitenburg, C., and Colcetti, G., 1997, Design Better Cerium-Based Oxidation Catalysts, CHEMTECH, 27, 32.

Woods, M. C., Gangwal, S. K., Jothimurugesan, K., and Harrison, D. P., 1990, The Reaction Between H_2S and Zinc Oxide-Titanium Oxide Sorbent: 1. Single Pellet Kinetic Studies, Industrial and Engineering Chemistry Research, 29, 1160.

Zamar, F., Travarelli, A., de Leitenburg, C., and Dolcetti, G., 1995, CeO_2-Based Solid Solutions with the Fluorite Structure as Novel and Effective Catalysts for Methane Combustion, Journal of the Chemical Society, Chemical Communications, 965.

Zeng, Y, Zhang, S., Groves, F. R., and Harrison, D. P., 1999, High Temperature Gas Desulfurization with Elemental Sulfur Production, Chemical Engineering Science, 54, 3007.

Zeng, Y., 1999a, Cerium Oxide as a Highly Effective and Durable High Temperature Desulfurization Sorbent, Ph. D. Dissertation, Louisiana State University.

Zeng, Y., Kaytakoglu, S., and Harrison, D. P., 2000, Reduced Cerium Oxide as an Efficient and Durable High Temperature Desulfurization Sorbent, Chemical Engineering Science, 55, 4893.

Zhou, Y., Phillips, R. J., and Switzer, J., 1995, Electrochemical Synthesis and Sintering of Nanocrystalline Cerium(IV) Oxide Powders, Journal of the American Ceramic Society, 78, 981.